

Table 1. Summary of Genes and Proteins on Human Chromosome X

identification level	database	identified/total	%	URL
Transcript	neXtProt	823/874	94.2%	http://www.nextprot.org
neXtProt	neXtProt	615/874	70.4%	http://www.proteinatlas.org/
	Peptide Atlas	396/874	45.3%	http://www.peptideatlas.org
	SRM Atlas	~19000/ ~20300	93.6% ^a	http://www.srmatlas.org
	GPM DB	657/862	76.2%	http://www.thegpm.org
Protein by Antibody	HPA	495/841	55.7%	http://www.proteinatlas.org
	Antibodypedia	722/874	82.6%	http://www.antibodypedia.com
Disorders associated ^b	neXtProt	195/874	22.3%	
	OMIM Gene Map	305/874	34.9%	http://omim.org/geneMap
	Genetics Home Reference	107/874	12.2%	http://ghr.nlm.nih.gov/chromosome/X/show/Conditions

^aEstimated based on all genes. ^bIncluding Dominant X-linked diseases (related gene): Vitamin D resistant rickets (X-linked hypophosphatemia, PHEX), Rett syndrome (MECP2), Fragile X syndrome (FMR1), Alport syndrome (COL4A5), etc. X-linked recessive inheritance: Color blindness (OPN1MW, OPN1LW), Hemophilia (F8, F9), Duchenne muscular dystrophy (DMD), X-linked agammaglobulinemia (BTK), Fabry disease (GLA), etc.

Region on the Y chromosome), determines male by inducing and developing the testis to produce a male hormone, androgen. On the chromosome X only a few of the 888 genes directly play a role in sex determination. One is the gene encoding androgen receptor on the chromosome X, indicating the importance of chromosome X in males and suggesting a cross-communication between chromosomes X and Y and also the significance of the androgen receptor in females.

Besides the sex-determining genes, genes in the neural system are uniquely clustered on chromosome X: NLGN3 (Neuroigin-3), NLGN4X (Neuroigin-4, X-linked), OPHN1 (Oligophrenin-1), PAK3 (Serine/threonine-protein kinase), FMR1 (fragile X mental retardation 1), MAG (myelin associated glycoprotein) and others. Proteins translated from these genes are essential for interaction or communication of neurons and are presumed to relate to the intelligence.² The important role of the X chromosome in brain function is also evident from the prevalence of X-linked forms of mental retardation.

The accumulation of immune system-related genes to chromosome X also attracts attention. CD40L (CD40 ligand), IL2RG (Cytokine receptor common subunit gamma), BTK (Tyrosine-protein kinase), F8 (Coagulation factor VIII), and F9 (Coagulation factor IX) are example of chromosome X genes that are involved in the immune system and coagulation system.³

The inactivation of chromosome X is a process by which one of the two copies of chromosome X in females is inactivated. The inactive X chromosome is transcriptionally silenced to form an inactive structure called heterochromatin. The choice of which X chromosome is inactivated is randomly occurring in each cell in mammals. The X-inactivation center on the X chromosome, which is essential to cause X-inactivation, contains four nontranslated RNA genes, Xist, Tsix, Jpx and Ftx, which are involved in X-inactivation.^{4,5}

2. Human Chromosome X-Proteins Identified by Mass Spectrometry (MS)

Information of genes on chromosome X and the proteins encoded by the genes has been collected in several databases (Table 1). In the neXtProt database (<http://www.nextprot.org>), 874 genes are presumed on chromosome X.¹ Among them, 823 (94.2%) genes have been identified at the transcript level and 615 (70.4%) genes have been demonstrated at the protein level by proteomics. In the other proteome databases, Peptide Atlas and GPM DB (Global Proteome Machine

database), 45.3 and 75.2%, respectively, of the genes on chromosome X are identified as proteins. However, these data indicate that more than 200 genes on chromosome X are still unclear whether they translate proteins or not. These unclear proteins are further confirmed by MS and immunohistochemistry using antibodies in this project.

3. Proteomes Identified by Antibody-based Methods

Collection and validation of antibodies against human proteins are progressing by Human Protein Atlas project.⁶ By using antibodies, localization of 495 (56.6%) chromosome X-proteins has been examined at cellular and subcellular levels in human body.

The Antibodypedia is a Web site providing datasheets of antibodies against human proteins from antibody providers (<http://www.antibodypedia.com>). In this collection, datasheets of antibodies against 722 (82.6%) chromosome X-proteins are currently shown although these antibodies have not always been well-characterized in the specificity or reactivity to the proteins for immunolocalization. The Chromosome X Project Consortium members will collect significant evidence of the presence or localization of the chromosome X-proteins from the literature or from their own research.

4. Diseases Associated with Chromosome X

A large number of genes (195 in the neXtProt database) in chromosome X have been demonstrated to associate with genetic disorders and hereditary diseases in humans (Table 1). One of the reasons is only one copy of chromosome X is active both in males (XY) and females (XX) (X-inactivation), resulting in prevalence of X-linked hereditary diseases.

It is estimated that about 10% of the genes (99 genes) encoded by the X chromosome are associated with a family of "CT antigen (cancer-testis antigen)" genes, which encode for markers found in both cancer cells as well as in the human testis (MAGE, GAGE, SSX, SPANX or other CT gene families).⁷

THE JAPAN CHROMOSOME X PROJECT

1. Selection of Tissues and Organs

Since preference in expression of chromosome X genes in neural and immune systems and the tissues (neural and immune systems or cancers and testis) has been demonstrated as described above, it is presumed that expression of chromosome X-proteins is also different among organs or tissues. Therefore, expression of chromosome X-proteins were searched in the kidney, brain, ovary and testis in the Human

Protein Atlas. As shown in Table 2, there was no significant preference in the expression among the organs. Therefore, the

Table 2. Identification of Chromosome X-Proteins in the Human Protein Atlas^a

	antibodies used	immunohistochemistry	
		strong (%)	weak (%)
Placenta	627	148 (23.6)	490 (78.1)
Kidney	900	149 (16.6)	654 (72.7)
Ovary	1180	160 (13.6)	825 (69.9)
Testis	1032	224 (21.7)	821 (79.6)
Brain	1112	159 (14.3)	776 (69.8)

^aPlacenta, kidney, ovary, testis and brain tissues were examined by immunohistochemistry using antibodies in the Human Protein Atlas (<http://www.proteinatlas.org/>). Numbers of antibodies used, stained the tissues strongly or more than weakly are shown (%).

Japan chromosome X project consortium preliminarily chose kidney, ovary, and breast as target sample tissues to look for chromosome X-proteins, which had not been well-identified yet because these organs had not been analyzed by other chromosome projects and our project members had already analyzed the proteomes of these organs more or less.

2. Collection of Protein Existence by MS

With informed consent, human kidney, ovary, breast tissues were obtained from patients when these organs or tissues were surgically removed for treatment of cancers. Kidneys were separated into cortex, medulla and glomerulus.⁸ More fine structured (proximal tubule, distal tubule, collecting duct, and others) kidney sections were microdissected from kidney sections by laser microdissection system for deeper and more comprehensive MS analysis of kidney nephron parts. Other organs are also considered for such in depth MS analysis.

Members of the Japan Chromosome X Project are interested in MS analysis of cancers^{9–12} and biofluids^{13,14} for biomarker discovery and understanding of pathophysiology of cancers. Other members are also focusing on analysis of protein modification such as phosphorylation or glycosylation and collect MS evidence of post-translational modifications of chromosome X-proteins in the target organs and others.¹⁵

Another approach to find possible tissue or organ sites was carried out to develop a search engine ("Transcript Localizer") to look at human microarray databases and to pick up sites where missing or unclear chromosome X genes are detected.

3. Collection of Protein Localization by Antibodies

Cellular localization of proteins, which would first be identified by MS in the target organs, was secondarily searched in the Human Protein Atlas database and the immunohistochemistry images were retrieved to combine to the data obtained by MS-based proteomics. A prototype of the human kidney proteome database has been opened to the public at the Web site of the HUPO Human Kidney and Urine Proteome Project (HKUPP) Initiative (www.hkupp.org/). The members of the chromosome X project also examined localization of MS-identified proteins in the target organs by immunohistochemistry to confirm the Human Protein Atlas data and the MS identification results. Our consortium will collect information on antibodies to the proteins, which are not provided by the Human Protein Atlas project, by searching in the Antibodypedia.

We are also developing an antibody search engine tool that looks for antibodies in open free access articles in the PubMed database and picks up antibodies to human proteins and collects the following information: name of companies providing antibodies and images obtained by the antibodies. Several different antibodies to one human protein were used in the past studies and the search engine collects information of all of these antibodies and will demonstrate antibody information in a rank order of number of articles in which the same antibody was used. This informs us which antibody is mostly used for a human protein in a community of scientists. Therefore, the tool was named "Antibody Ranker". We believe this tool provides valuable information for researchers who are looking for antibodies for human proteins. Efficiency of the Antibody Ranker is also validated by selecting antibodies for immunohistochemistry in the chromosome X project.

4. Resources and Tools Developed from the Chromosome X Project

The Human Gene and Protein Database (HGPD; <http://www.HGPD.jp/>) launched in 2008 is a unique resource storing 43249 human Gateway entry clones constructed from the open reading frames (ORFs) of full-length human cDNA, which is the largest in the world.¹⁶ Since the set of these clones are used for recombinant human protein synthesis by the wheat germ cell-free protein synthesis system, this resource is named the Human Proteome Expression Resource (HuPEX).¹⁷ The recombinant protein resource has covered more than 85% of human proteins encoded by 20300 genes.

All synthesized proteins (approx. 18000) have been intensively analyzed by MS after trypsinization and MS/MS information of individual peptides from the proteins has been collected as a database for selection of peptides and MRM (multiple reaction monitoring) transitions. This provides us information to select peptides and MS/MS transitions for MRM (information-based MRM, iMRM) and also resources of reference peptides for quantitation of proteins in the target tissues.

CONCLUSION

Current status and future plans of the Japan human chromosome X project are summarized in Figure 1 .. Collaboration and cooperation with other chromosome

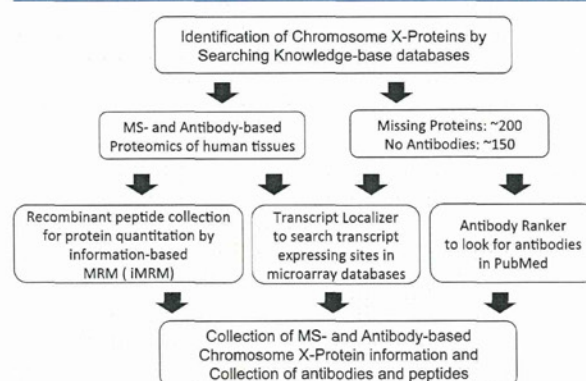


Figure 1. Workflow of Japan Chromosome X Project. Shown here is a strategy from basic collection of knowledge-base proteomics data to final completion of chromosome X proteome data and resource collection done by Japan Chromosome X Project Consortium.

projects in the Chromosome-centric Human Proteome Project, especially chromosome Y and with other Biology/Disease Human Proteome projects, need to be facilitated to complete the Human Proteome Project.

AUTHOR INFORMATION

Corresponding Author

*E-mail: tdsymm@med.niigata-u.ac.jp. Tel: +81-25-227-2151. Fax: +81-25-227-0768.

Notes

The authors declare no competing financial interest.

ACKNOWLEDGMENTS

This study was supported by a Grant-in-Aid for Scientific Research (B) to T.Y. ((21390262) from Japan Society for Promotion of Science and by a Grant-in-Aid for Strategic Research Project to T.Y. (500460) from Ministry of Education, Culture, Sports, Science and Technology, Japan and by a Grant-in-Aid for Diabetic Nephropathy and Nephrosclerosis Research from the Ministry of Health, Labor and Welfare of Japan.

REFERENCES

- (1) Lane, L.; Argoud-Puy, G.; Britan, A.; Cusin, I.; Duek, P. D.; Evalet, O.; Gateau, A.; Gaudet, P.; Gleizes, A.; Masselot, A.; Zwahlen, C.; Bairoch, A. neXtProt: a knowledge platform for human proteins. *Nucleic Acids Res.* **2011**, *40*, D76–83.
- (2) Nguyen, D. K.; Disteché, C. M. High expression of the mammalian X chromosome in brain. *Brain Res.* **2006**, *1126*, 46–9.
- (3) Libert, C.; Dejager, L.; Pinheiro, I. The X chromosome in immune functions: when a chromosome makes the difference. *Nat. Rev. Immunol.* **2010**, *10*, 594–604.
- (4) Brockdorff, N. Chromosome silencing mechanisms in X-chromosome inactivation: unknown unknowns. *Development* **2011**, *138*, 5057–65.
- (5) Reinius, B.; Shi, C.; Hengshuo, L.; Sandhu, K. S.; Radomska, K. J.; et al. Female-biased expression of long non-coding RNAs in domains that escape X-inactivation in mouse. *BMC Genomics* **2010**, *11*, 614.
- (6) Uhlen, M.; Oksvold, P.; Fagerberg, L.; Lundberg, E.; Jonasson, K.; Forsberg, M.; Zwahlen, M.; Kampf, C.; Wester, K.; Hober, S.; Wernerus, H.; Björling, L.; Pontén, F. Towards a knowledge-based Human Protein Atlas. *Nat. Biotechnol.* **2010**, *28*, 1248–50.
- (7) Ross, M.; Grafham, D. V.; Coffey, A. J.; Scherer, S.; McLay, K.; et al. The DNA sequence of the human X chromosome. *Nature* **2005**, *434*, 325–37.
- (8) Miyamoto, M.; Yoshida, Y.; Taguchi, I.; Nagasaka, Y.; Tasaki, M.; et al. In-depth proteomic profiling of the normal human kidney glomerulus using two-dimensional protein prefractionation in combination with liquid chromatography-tandem mass spectrometry. *J. Proteome Res.* **2007**, *6*, 3680–90.
- (9) Masuishi, Y.; Arakawa, N.; Kawasaki, H.; Miyagi, E.; Hirahara, F.; Hirano, H. Wild-type p53 enhances annexin IV gene expression in ovarian clear cell adenocarcinoma. *FEBS J.* **2011**, *27*, 1470–83.
- (10) Muraoka, S.; Kume, H.; Watanabe, S.; Adachi, J.; Kuwano, M.; et al. Strategy for SRM-based verification of biomarker candidates discovered by iTRAQ method in limited breast cancer tissue samples. *J. Proteome Res.* **2012**, *11*, 4201–10.
- (11) Ono, M.; Kamita, M.; Murakoshi, Y.; Matsubara, J.; Honda, K.; et al. Biomarker discovery of pancreatic and gastrointestinal cancer by 2DICAL: 2-dimensional image-converted analysis of liquid chromatography and mass spectrometry. *Int. J. Proteomics.* **2012**, *2012*, 897412.
- (12) Sugihara, Y.; Taniguchi, H.; Kushima, R.; Tsuda, H.; Kubota, D.; et al. Proteomic-based identification of the APC-binding protein EB1 as a candidate of novel tissue biomarker and therapeutic target for colorectal cancer. *J. Proteomics* **2012**, *75*, 5342–55.
- (13) Kawashima, Y.; Fukutomi, T.; Tomonaga, T.; Takahashi, H.; Nomura, F.; Maeda, T.; Kodaera, Y. High-yield peptide-extraction method for the discovery of subnanomolar biomarkers from small serum samples. *J. Proteome Res.* **2010**, *9*, 1694–705.
- (14) Kobayashi, M.; Matsumoto, T.; Ryuge, S.; Yanagita, K.; Nagashio, R.; et al. CAXII Is a sero-diagnostic marker for lung cancer. *PLoS One* **2012**, *7*, e33952.
- (15) Imamura, H.; Wakabayashi, M.; Ishihama, Y. Analytical strategies for shotgun phosphoproteomics: status and prospects. *Semin. Cell Dev. Biol.* **2012**, *23*, 836–42.
- (16) Goshima, N.; Kawamura, Y.; Fukumoto, A.; Miura, A.; Honma, R.; et al. Human protein factory for converting the transcriptome into an in vitro-expressed proteome. *Nat. Methods* **2008**, *5*, 1011–7.
- (17) Maruyama, Y.; Kawamura, Y.; Nishikawa, T.; Isogai, T.; Nomura, N.; Goshima, N. HGPS: Human Gene and Protein Database, 2012 update. *Nucleic Acids Res.* **2012**, *40*, D924–9.

A Strategy for Large-Scale Phosphoproteomics and SRM-Based Validation of Human Breast Cancer Tissue Samples

Ryohei Narumi,^{#,†} Tatsuo Murakami,^{#,†} Takahisa Kuga,[†] Jun Adachi,[†] Takashi Shiromizu,[†] Satoshi Muraoka,[†] Hideaki Kume,[†] Yoshio Kodera,^{‡,§} Masaki Matsumoto,^{||} Keiichi Nakayama,^{||} Yasuhide Miyamoto,[⊥] Makoto Ishitobi,[¶] Hideo Inaji,[¶] Kikuya Kato,[∇] and Takeshi Tomonaga^{*,†,§}

[†]Laboratory of Proteome Research, National Institute of Biomedical Innovation, Osaka, Japan

[‡]Laboratory of Biomolecular Dynamics, Department of Physics, Kitasato University School of Science, Kanagawa, Japan

[§]Clinical Proteomics Research Center, Chiba University Hospital, Chiba, Japan

^{||}Department of Molecular and Cellular Biology, Medical Institute of Bioregulation, Kyushu University Fukuoka, Japan

[⊥]Department of Immunology, Osaka Medical Center for Cancer and Cardiovascular Diseases, Osaka, Japan

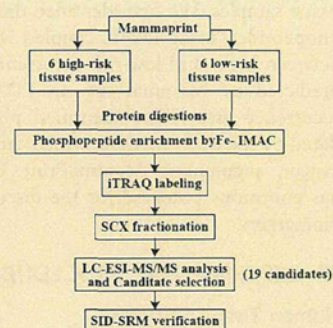
[¶]Department of Breast and Endocrine Surgery, Osaka Medical Center for Cancer and Cardiovascular Diseases, Osaka, Japan

[∇]Research Institute, Osaka Medical Center for Cancer and Cardiovascular Diseases, Osaka, Japan

Supporting Information

ABSTRACT: Protein phosphorylation is a key mechanism of cellular signaling pathways and aberrant phosphorylation has been implicated in a number of human diseases. Thus, approaches in phosphoproteomics can contribute to the identification of key biomarkers to assess disease pathogenesis and drug targets. Moreover, careful validation of large-scale phosphoproteome analysis, which is lacking in the current protein-based biomarker discovery, significantly increases the value of identified biomarkers. Here, we performed large-scale differential phosphoproteome analysis using IMAC coupled with the isobaric tag for relative quantification (iTRAQ) technique and subsequent validation by selected/multiple reaction monitoring (SRM/MRM) of human breast cancer tissues in high- and low-risk recurrence groups. We identified 8309 phosphorylation sites on 3401 proteins, of which 3766 phosphopeptides (1927 phosphoproteins) were able to be quantified and 133 phosphopeptides (117 phosphoproteins) were differentially expressed between the two groups. Among them, 19 phosphopeptides were selected for further verification and 15 were successfully quantified by SRM using stable isotope peptides as a reference. The ratio of phosphopeptides between high- and low-risk groups quantified by SRM was well correlated with iTRAQ-based quantification with a few exceptions. These results suggest that large-scale phosphoproteome quantification coupled with SRM-based validation is a powerful tool for biomarker discovery using clinical samples.

KEYWORDS: phosphoproteome, iTRAQ, SRM, mammaprint, breast cancer tissue



INTRODUCTION

Protein phosphorylation is a key regulator of cellular signal-transduction processes, and its deregulation is involved in the onset and progression of various human diseases, such as cancer, inflammation, and metabolic disorders.^{1–4} Recent advances in proteomics, especially phosphopeptide enrichment strategies⁵ and improved isotope labeling,^{6,7} enabled not only the identification of up to several thousands of site-specific phosphorylation events within one large-scale analysis^{8–18} but also accurate quantification of the phosphopeptides/proteins.^{19–22} Immobilized metal ion affinity chromatography (IMAC) is a widely used affinity-based technique for the enrichment of phosphopeptides prior to MS analysis. Metal ions are chelated to nitrilotriacetic acid- or iminodiacetic acid-coated beads, forming a stationary phase to which negatively charged phosphopeptides in a mobile phase can bind.⁵ Isotope labeling techniques are classified into two groups, metabolic labeling and chemical

labeling; representative examples of each label are stable isotope labeling by amino acids in cell culture (SILAC)⁶ and isobaric tag for relative and absolute quantification (iTRAQ), respectively.

This large-scale phosphoproteome analysis has recently been applied to biomarker discovery using cell culture and tumor model mice. Zanivan et al. analyzed the phosphoproteome of tumor tissues of melanoma model mice and identified more than 5600 phosphorylation sites on 2250 proteins, which included many hits from pathways important in melanoma.²³ Despite such a large effort to generate a list of biomarker candidates, extensive validation by other methods is needed for application as a biomarker. Currently, the most commonly used approach for verification is Western blotting and sandwich enzyme-linked immunosorbent assay (ELISA); however, antibody

Received: June 18, 2012

Published: September 17, 2012

reagents of sufficient specificity and sensitivity for the assays are generally not available, especially for phosphoproteins. Also, the high cost and long development time required to generate high-quality reagents are limiting factors; therefore, the development of an alternate method for verification with high reproducibility and throughput is needed to improve the success rate of approved biomarkers.²⁴

A new mass spectrometry-based analytical platform called selected reaction monitoring (SRM) or multiple reaction monitoring (MRM) is a very sensitive technique for the quantification of targeted proteins and peptides, which makes it possible to verify biomarker candidate proteins.²⁵ Suitable sets of precursor and fragment ion masses for a given peptide, called SRM transitions, constitute definitive mass spectrometry assays that identify peptides and the corresponding proteins. More recently, SRM using stable isotope peptides has been adapted to measure the concentrations of candidate protein biomarkers in cell lysates as well as human plasma and serum.^{26–29} Consequently, SRM technology shows potential to bridge the gap between the generation of candidate lists and their verification in biological specimens.

In this study, we applied large-scale phosphoproteome analysis and SRM-based quantitation to develop a strategy for the systematic discovery and validation of biomarkers using tissue samples. We first identified differentially expressed phosphopeptides, using IMAC coupled with the iTRAQ technique, between high- and low-risk recurrence groups of breast cancer predicted by MammaPrint, an FDA-approved breast cancer recurrence assay. The identified phosphopeptides were validated by the SRM method, which can find biomarkers of breast cancer, augmenting MammaPrint. This systematic approach has enormous potential for the discovery of bona fide disease biomarkers.

■ EXPERIMENTAL PROCEDURES

Human Tissue Samples

Tumor tissue samples were obtained from 12 patients with breast cancer at Osaka Medical Center for Cancer & Cardiovascular Diseases. Information about the 12 patients is summarized in Supporting Information Table S1. Tissue samples were frozen in liquid nitrogen and stored at -80°C until analysis. The patients were classified into good (low-risk) or poor (high-risk) prognosis groups using MammaPrint, as described previously.³⁰ Written informed consent was obtained from each patient before surgery. The protocol was approved by the ethics committees of the Proteome Research Center, National Institute of Biomedical Innovation and the Osaka Medical Center for Cancer & Cardiovascular Diseases.

Protein Extraction and Digestion

Protein extraction and proteolytic digestion were performed using a phase-transfer surfactant protocol.³¹ Tissue samples or pellets of cultured cells were homogenized by sonication in a lysis buffer [12 mM sodium deoxycholate, 12 mM sodium *N*-lauroylsarcosinate, 50 mM ammonium bicarbonate, and PhosSTOP phosphatase inhibitor cocktail (Roche Applied Science, Indianapolis, IN, USA)]. Protein concentration was determined by a DC protein assay kit (Bio-Rad Laboratories, Hercules, CA, USA). A sample of 2 mg (for iTRAQ) or 500 μg (for SRM) of extracted proteins was reduced with 10 mM dithiothreitol (DTT), alkylated with 50 mM iodoacetamide (IAA), and diluted by 5 times with 50 mM ammonium bicarbonate solution, and sequentially digested by 1:100 (w/w)

LysC (Wako Pure Chemical Industries, Osaka, Japan) for 8 h at 37°C and 1:100 (w/w) trypsin (proteomics grade; Roche) for 12 h at 37°C . An equal volume of an organic solvent, ethyl acetate, was added to the digested samples; the mixtures were acidified by 1% trifluoroacetic acid (TFA) and vortexed to transfer the detergents to the organic phase. After centrifugation, the aqueous phase containing peptides was collected.

Enrichment of Phosphopeptides

Phosphopeptide enrichment was performed using immobilized Fe (III) affinity chromatography [Fe-IMAC], as described previously.³² The Fe-IMAC resin was prepared from Probond (Nickel-Chelating Resin; Invitrogen, Carlsbad, CA, USA) by substituting Ni^{2+} on the resin with Fe^{3+} . Ni^{2+} was released from Probond upon treatment with 50 mM EDTA-2Na, and then Fe^{3+} was chelated to ion-free resin upon incubation with 100 mM FeCl_3 in 0.1% acetic acid. Fe-IMAC resin was packed into an open column for large-scale enrichment or on an Empore C18 disk in a 200- μL pipet tip for small-scale enrichment.³³ After equilibration of the resin with loading solution (60% acetonitrile/0.1% TFA), peptide mixture was loaded onto the IMAC column (200 μg total peptides per 100 μL resin). After washing with loading solution (9 times volume of IMAC resin) and 0.1% TFA (3 times volume of IMAC resin), phosphopeptides were eluted by 1% phosphoric acid (2 times volume of IMAC resin).

iTRAQ Analysis

iTRAQ Labeling. Enriched phosphopeptides were labeled with isobaric tags for relative and absolute quantification reagents (iTRAQ 4 plex; Applied Biosystems, Foster City, CA, USA) according to the manufacturer's instructions. Phosphopeptide mixtures desalted with C18 Stage-Tips were incubated in iTRAQ reagents for 1 h. iTRAQ 115, 116, and 117 were used for labeling individual samples, and iTRAQ 114 was used as the reference sample, a mixture of aliquots of all samples. The reaction was terminated by the addition of an equal volume of distilled water. The labeled samples were combined, acidified by TFA, and desalted with C18-Stage Tips. Four sets of iTRAQ experiments were performed to compare the phosphorylation profiles of 12 tissue samples

Strong Cation Exchange Chromatography (SCX). The labeled peptides were fractionated using an HPLC system (Shimadzu Prominence UFLC) fitted with an SCX column (50 mm \times 2.1 mm, 5 μm , 300 \AA , ZORBAX 300SCX; Agilent Technology). The mobile phases consisted of buffers A [25% acetonitrile and 10 mM KH_2PO_4 (pH 3)] and B [25% acetonitrile, 10 mM KH_2PO_4 (pH 3), and 1 M KCl]. The labeled peptides were dissolved in 200 μL of buffer A and separated at a flow rate of 200 $\mu\text{L}/\text{min}$ using a four-step linear gradient: 0% B for 30 min, 0–10% B in 15 min, 10–25% B in 10 min, 25–40% B in 5 min, and 40–100% B in 5 min, and then 100% B for 10 min. Thirty fractions were collected and desalted with C18-Stage Tips.

LC-MS/MS Analysis. Fractionated peptides were analyzed by an LTQ-Orbitrap XL or Velos mass spectrometer (Thermo Fisher Scientific, Bremen, Germany) equipped with a nanoLC interface (AMR, Tokyo, Japan), a nanoHPLC system (Michrom Paradigm MS2), and an HTC-PAL autosampler (CTC Analytics, Zwingen, Switzerland). The analytical column was made in-house by packing L-column2 C18 particles [Chemical Evaluation and Research Institute (CERI), Japan] into a self-pulled needle (200 mm length \times 100 μm inner diameter). The mobile phases consisted of buffers A (0.1% formic

acid and 2% acetonitrile) and B (0.1% formic acid and 90% acetonitrile). Samples dissolved in buffer A were loaded onto a trap column (0.3×5 mm, L-column ODS; CERI). The nanoLC gradient was delivered at 500 nL/min and consisted of a linear gradient of buffer B developed from 5 to 30% B in 135 min. A spray voltage of 2000 V was applied.

Full MS scans were performed using the orbitrap mass analyzer (scan range 350–1500 m/z , with 30000 fwhm resolution at 400 m/z). The three (LTQ XL) or five (LTQ Velos) most intense precursor ions were selected for the MS/MS scans, which were performed using collision-induced dissociation (CID) and higher energy collision-induced dissociation (HCD, 7500 fwhm resolution at 400 m/z) for each precursor ion. The dynamic exclusion option was implemented with a repeat count of 1 and exclusion duration of 60 s. The values of automated gain control (AGC) were set to 5.00×10^5 for full MS, 1.00×10^4 for CID MS/MS, and 5.00×10^4 for HCD MS/MS. The normalized collision energy values were set to 35% for CID and 50% for HCD.

The CID and HCD raw spectra were extracted and searched separately against the human IPI database (version 3.67) combined with the reverse-decoy database using Proteome Discoverer 1.3 (Thermo Fisher Scientific) and Mascot v2.3. The precursor mass tolerance was set to 3 ppm, and fragment ion mass tolerance was set to 0.6 Da for CID and 0.01 Da for HCD. The search parameters allowed one missed cleavage for trypsin, fixed modifications (carbamidomethylation at cysteine and iTRAQ labeling at lysine and the N-terminal residue), and variable modifications (oxidation at methionine, iTRAQ labeling at tyrosine, and phosphorylation at serine, threonine, and tyrosine). In the workflow of Proteome Discoverer 1.3, following the Mascot search, the phosphorylated sites on the identified peptides were assigned again using the PhosphoRS algorithm, which calculated the possibility of the phosphorylated site from the spectra matching the identified peptides.³⁴ The score threshold for peptide identification was set at 1% false-discovery rate (FDR) and 75% phosphoRS site probability. Peptides identified at a threshold with 5% FDR were also accepted in the case that a peptide with the same sequence was identified at a threshold with 1% FDR in any other three iTRAQ experiments.

The iTRAQ quantitation values were automatically calculated on the basis of the intensity of the iTRAQ reporter ions in the HCD scans using Proteome Discoverer. Quantitation of peptides identified from CID scans was performed using the reporter ion information extracted from the HCD spectra of the same precursor peptide. In the case that peptides with the same sequence were identified repeatedly from different precursor peptides in the same iTRAQ experiment, the median of their quantitation values was calculated. For comparison among 4 sets of iTRAQ experiments, iTRAQ quantitation values of individual samples (iTRAQ 115, 116, and 117) were normalized with the values of the reference sample (iTRAQ 114) in each iTRAQ experiment.

SRM Analysis

Stable Isotope-Labeled Peptides. For SRM measurement of the 19 targeted phosphopeptides, stable isotope-labeled peptides (SI peptides, crude grade) were synthesized (Thermo Fisher Scientific, Ulm, Germany). A single lysine, arginine, or alanine was replaced by isotope-labeled lysine ($^{13}\text{C}_6$, 98%; $^{15}\text{N}_2$, 98%), arginine ($^{13}\text{C}_6$, 98%; $^{15}\text{N}_4$, 98%), or alanine ($^{13}\text{C}_3$, 98%; $^{15}\text{N}_1$, 98%). The SI peptides were dissolved

in distilled water at a concentration of $1 \mu\text{g}/\mu\text{L}$ and stored at -80°C . A mixture of these SI peptides was added to each sample during the period between tryptic digestion and detergent extraction processes in the PTS protocol.

Setting SRM Transition. First, the mixture of SI peptides was analyzed by LC-MS/MS using LTQ-Orbitrap XL (CID mode), and an msf file was generated using Proteome Discoverer and Mascot. The msf file was opened with Pinpoint software (version 2.3.0; Thermo Scientific), and a list of MS/MS fragment ions derived from SI peptides was generated. Four MS/MS fragment ions were selected for SRM transitions of each targeted peptide based on the following criteria: y -ion series, strong ion intensity, at least 2 amino acids in length, and no signature of neutral loss.

LC-SRM. Protein extracts were digested, spiked with the SI peptides, and subjected to phospho-enrichment with IMAC. The enriched phosphopeptides dissolved in 2% acetonitrile solution containing 0.1% TFA and 25 $\mu\text{g}/\text{mL}$ of EDTA were analyzed by a TSQ-Vantage triple quadrupole mass spectrometer (Thermo Fisher Scientific) equipped with the LC system mentioned above. The parameters of the instrument were set as follows: 0.002 m/z scan width, 0.7 fwhm Q1 resolution, 1 s cycle time, and 1.8 mTorr gas pressure. The S-lens voltage was set to a normalized value determined using polytyrosine and angiotensin II as references. Collision energy (CE) was optimized for every SRM transition around the theoretical value calculated according to the following formulas: $\text{CE} = 0.044(m/z) + 5.5$ for doubly charged precursor ions and $\text{CE} = 0.051(m/z) + 0.55$ for triply charged precursor ions. If the theoretical value was over 35 eV, the value was set to 35 eV. The nanoLC gradient was delivered at 300 nL/min and consisted of a linear gradient of mobile phase B developed from 5 to 23% B in 45 min. A spray voltage of 1800 V was applied. Data were acquired in time-scheduled SRM mode (retention time window: 8 min). Targeted phosphopeptides were quantified using Pinpoint. The peak area in the chromatogram of each SRM transition was calculated, and the values of endogenous targeted peptides were normalized to those of the corresponding SI peptides. SRM transition peak with more than 3 times the standard deviation of the average value of the blanks was used for quantitation. We checked that ratios among the peak areas of individual SRM transitions for each targeted phosphopeptide were comparable to those of the corresponding SI peptide.

Western Blot Analysis

Proteins were separated by electrophoresis on 5–20% gradient gels (DRC, Tokyo, Japan) and transferred to an Immobilon-P Transfer membrane ($0.45 \mu\text{m}$) (Millipore, Bedford, MA, USA) in a tank-transfer apparatus. The membrane was blocked with Immuno Block (DS Pharma Biomedical Co., Ltd., Osaka, Japan). Anti-Mucin-1 antibody (Thermo Scientific, Rockford, IL, USA), diluted 1:1000 in blocking buffer, was used as the primary antibody. Goat anti-Armenian Hamster IgG horseradish peroxidase (Jackson ImmunoResearch Laboratories, Inc., West Grove, PA, USA), diluted 1:5000 in blocking buffer, was used as the secondary antibody. Antigens on membranes were detected with enhanced chemiluminescence detection reagents (GE Healthcare, Little Chalfont, Buckinghamshire, U.K.).

RESULTS

iTRAQ Analysis of Phosphoproteins Prepared from Breast Cancer Tissues and Identification of Potential Prognostic Biomarkers

Recent advances in phosphoproteomics enabled not only the identification of up to several thousands of site-specific phosphorylation events within one large-scale analysis,^{8–18} but also the accurate quantification of phosphopeptides/proteins.^{19–22} This large-scale phosphoproteome analysis has recently been applied to biomarker discovery using cell culture, a tumor model mouse,²³ and human tissues.³⁵ In order to discover candidate prognostic biomarkers for breast cancer, we identified and validated the differentially expressed phosphoproteins in breast cancer tissues from 12 patients who had been classified by MammaPrint into the high- or low-risk group, as shown in the strategy in Figure 1. To identify the differentially expressed phosphoproteins, quantitative phosphoproteomics of the 12 samples of breast cancer tissue was performed by iTRAQ analysis combined with enrichment of phosphopeptides (Supporting Information Figure S1). In each experiment, the

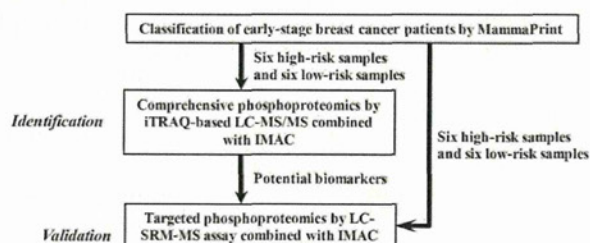


Figure 1. Strategy for the discovery of candidate prognostic biomarkers for breast cancer using iTRAQ-based proteomic analysis and SRM-based proteomic analysis. In order to discover biomarker candidates, we quantitatively compared protein phosphorylation between 12 breast cancer tissues that were classified into a high- or low-risk group by MammaPrint using iTRAQ-based proteomic analysis combined with IMAC. Subsequently, the differentially expressed phosphoproteins were validated using SRM-based proteomic analysis combined with IMAC.

sample prepared from the 12 individual samples of tissue lysate (Pooled sample) was always used as the internal standard labeled by iTRAQ reagent with 114-reporter. Meanwhile, three individual samples were labeled with iTRAQ reagents having 115-, 116- and 117-reporters. The pooled and three individual samples were each processed into peptide mixtures and applied to Fe-IMAC to enrich the phosphopeptides. The resulting samples were labeled with iTRAQ reagents followed by mixing the four samples. The iTRAQ-labeled sample was fractionated into 30 fractions by SCX chromatography, and the fractions were analyzed by LC-MS/MS using LTQ Orbitrap XL or LTQ Orbitrap Velos. In each experiment, 3897, 3873, 5067, and 6371 unique phosphopeptides were identified at FDR <1% (Table 1A, Supporting Information Figure S2). All 9267 unique phosphopeptides (FDR <1%) were identified in all experiments (Table 1B, Supporting Information Table S2), and those peptides corresponded to 8309 unique phosphorylated sites (serine: 7139 sites, threonine: 1049 sites, tyrosine: 121 sites) on 3401 proteins (Table 1B). In all the identified phosphopeptides, we quantitatively compared those that were repeatedly identified in more than 3 experiments. A total of 3766 unique phosphopeptides were compared (Table 1B, Supporting Information Table S3). Thresholds set for *p* values (≤ 0.1) and fold changes (≥ 2) were used as criteria to filter comparison data sets. Phosphopeptides (phosphoproteins) for a significance difference were 133 (117) in iTRAQ analysis (Table 2, Supporting Information Table S4).

Verification of Phosphopeptide Abundance

Biomarkers discovered by large-scale phosphoproteomics are often difficult to validate because highly specific antibodies for the phosphoproteins are not available. In order to validate biomarker candidate phosphoproteins discovered by iTRAQ-based

Table 2. Number of Phosphopeptides with Significant Difference between Two Groups by iTRAQ Analysis

ratio, <i>p</i> -value (high vs low risk)	phosphoprotein	phosphopeptide
>2.0 (<i>p</i> < 0.1)	53	58
<0.5 (<i>p</i> > 0.1)	64	75
total	117	133

Table 1. Analyzed Samples and the Number of Identified Phosphopeptides in iTRAQ-Based Proteomic Analysis

		A ^a					
		iTRAQ					
# of experiment		114	115	116	117	unique phosphopeptides	mass spectrometer
1	Pool		H01	H02	L10	3897	LTQ Orbitrap XL
2	Pool		L11	L12	H03	3873	LTQ Orbitrap XL
3	Pool		H04	L13	H05	5067	LTQ Orbitrap XL
4	Pool		L14	H6	L15	6371	LTQ Orbitrap Velos
		B ^b					
		unique phosphoproteins	unique phosphopeptides		unique phosphorylation sites		
# of identification in all experiments		3401	9267		8309	Ser: 7139 Thr: 1049 Tyr: 121	
# of those quantitatively compared		1927	3766		3476	Ser: 3102 Thr: 350 Tyr: 24	

^aThe analyzed samples and the number of identified phosphopeptides in each experiment of iTRAQ analysis. ^bThe total number of identified phosphoproteins, phosphopeptides and phosphorylation sites in all experiments of iTRAQ analysis, and the number of those used for quantitative comparison.

Table 3. iTRAQ-Based Relative Quantification of Phosphopeptides^a

gene symbol	uniprot accession	protein name	targeted phosphopeptide	phosphorylated site	high/low ratio	T.TEST	H01 (Ex1)	H02 (Ex1)	H03 (Ex 2)	H04 (Ex 3)	H05 (Ex 3)	H06 (Ex 4)	L10 (Ex1)	L11 (Ex 2)	L12 (Ex 2)	L13 (Ex 3)	L14 (Ex 4)	L15 (Ex 4)	
RPL23A	P62750	60S ribosomal protein L23a	IRTpSPTFR	S43	6.78	0.0532	22.34	4.86	3.43	24.39	31.05	2.83	0.85	4.18	0.98	1.25	2.1	2.81	
TOP2A	P11388-1	Putative uncharacterized protein; TOP2A	VPDEEENEepSDNEK	S1142	4.17	0.0156	2.39	0.63	1.56	3.06	1.64	0.83	0.75	0.12	0.21	0.85	0.3	0.64	
MX1	P20591	Interferon-induced GTP-binding protein Mx1	WpSEVDIAK	S4	4.11	0.0642	0.87	0.2	2.98	1.69	0.39	1.96	0.07	0.49	0.5	0.12	0.27	0.31	
CDK1	P06493																		
CDK2	P24941	Cell division protein kinase 1/2/3	IGEGpTYGWYK	T14	3.56	0.0966	1.45	0.17	4.5	3.38	0.2	3.25	0.11	0.34	0.48	0.01	1.02	1.08	
CDK3	Q00526																		
BRCA1	P38398-1	Breast cancer type1 susceptibility protein	NYPpSQEELIK	S1524	3.47	0.0561	0.76	1.14	2.57			0.61	0.46	0.43	0.27		0.28	0.39	
LMO7	Q8WW11	LIM domain only protein 7	pSYTSDLQK	S417	2.8	0.0156	0.78	3.11	1.97	1.88	2.49	1.1	0.43	0.91	1.1	0.29	0.43	0.5	
ALG3	Q92685	Dolichyl-P-Man:Man(5)GlcNAc (2)-PP-dolichyl mannosyltransferase	SGpSAAQAEGLCK	S13	2.4	0.0099	3.59	2.07	1.68	2.3	1.93	4.06	0.85	0.96	0.67	0.11	1.57	1.38	
PDSSA	Q29RF7-1	Sister chromatid cohesion protein PDSS homolog A	IISVpTPVK	T1208	2.26	0.0269	1.06	0.71	2.17	2.2	1	1.23	0.38	0.51	0.8	0.13	0.83	0.76	
CCR1	P32246	C-C chemokine receptor type 1	VSSTSPSTGEHELpSAGF	S352	2.2	0.0052	1.31	1.01	0.73	1.6	0.91	1.71	0.4	0.45	0.71	0.58	0.67	0.48	
MCM2	P49736	DNA replication licensing factor MCM2	GLLYDpSDEEDEERPAR	S139	2.2	0.0414	1.44	0.85	2.67	2.32	1.14	0.94	1.09	0.55	0.64	0.72	0.46	0.81	
CDK1	P06493																		
CDK2	P24941	Cell division protein kinase 1/2/3	IGEGTpYGWYK	Y15	2.09	0.0451	3.6	1.03	2.36	3.31	2.4	0.97	139	1.06	1	0.16	0.67	1.32	
CDK3	Q00526																		
MPZL1	095297-1	Myelin protein zero-like protein 1	SESWpYADIR	Y263	0.48	0.0088	0.42	0.96	0.98	0.57	1.09	0.75	1.66	1.5	1.06	0.22	1.5	2.63	
NCOR1	O75376-1	Nuclear receptor co repressor 1	NQQLARppSQEEK	S509	0.44	0.0096			0.5	0.38	0.58	0.65		0.9	1.67	0.91	1.14	1.05	
KRT8	P05787	Keratin, type II cytoskeletal 8	YEELQpSLAGK	S291	0.43	0.0126	0.64	0.29	0.74	0.63	0.7	0.6	1.91	0.96	0.81	0.86	2.21	1.14	
MUC1	P15941-1	Mucin-1	YVPPSSTDRpSPYEK	S1227	0.42	0.009	0.63	0.46	0.72			0.64	1.02	1.1	2.03		1.84	1.28	
PKP2	Q99959-1	Plakophilin-2	LELpSPDSSPER	S151	0.41	0.0439	0.07	0.27	0.16	0.48	0.34	0.3	1.11	0.32	0.22	5.96	0.84	0.78	
INADL	Q8NI35-1	InaD-like protein	LFDDApSVDEPR	S645	0.4	0.0001	0.49	0.27	0.49	0.52	0.38	0.5	1.14	1.22	1.22	1.18	0.7	1.19	
MKL2	Q9ULH7-4	MKL/myocardin-like protein 2	EELpSPISK	S882	0.39	0.0074	0.61	0.44	0.77	0.28	0.34	0.36	1.21	0.79	1.98	0.74	0.99	0.94	
SHROOM3	Q8TF72-1	shroom family member 3 protein	pSPENSPVVKPK	S439	0.35	0.0226	0.76	0.34	0.69	0.47	0.86	0.24	3.14	1.29	1.18	1.04	0.81	1.62	

^aEx: number of iTRAQ experiments.

phosphoproteomics, the identified phosphoproteins were validated by the SRM method. Of the 117 phosphopeptides with a significant difference, we selected 19 phosphopeptides for the SRM assay (Table 3), including the following peptides that showed greater changes in phosphorylation: 60S ribosomal protein L23a (fold change: 6.78), interferon-induced GTP-binding protein Mx1 (4.11), LIM domain-only protein 7 (2.80), shroom family member 3 protein (0.35), InaD-like protein (0.40), plakophilin-2 (0.41) and peptides of the protein that were previously reported to indicate a relationship with a poor prognosis or malignancy of breast cancer: DNA topoisomerase 2- α (4.17),^{36,37} breast cancer type 1 susceptibility protein (3.47),^{38–40} cell division protein kinase 1/2/3 (3.56/2.09),⁴¹ DNA replication licensing factor MCM2 (2.20),⁴² sister chromatid cohesion protein PDS5 homologue A (2.26),⁴³ mucin-1 (0.42),^{44,45} keratin, type II cytoskeletal 8 (0.43),^{46,47} MKL/myocardin-like protein 2 (0.39),⁴⁸ nuclear receptor corepressor 1 (0.44),^{49,50} and the peptide of the membrane proteins: dolichyl-P-Man:Man(5)GlcNAc(2)-PP-dolichyl mannosyltransferase (2.40), C–C chemokine receptor type 1 (2.20), myelin protein zero-like protein 1 (0.48). The SRM study is described in detail in Supporting Information Figure S1. The SRM transitions of each targeted peptide and CE were optimized with SI peptides (Supporting Information Table S5). The breast cancer tissues were treated with the phase-transfer surfactant protocol and spiked with SI peptides followed by phosphopeptide enrichment using Fe-IMAC, as described in the Experimental Procedures. Quantification of a target phosphopeptide was based on the following criteria: (i) the signal-to-noise ratio of transition was greater than 10; (ii) the ratio of each transition peak of the endogenous phosphopeptide was equal to that of the corresponding SI peptide; (iii) the elution time of the endogenous phosphopeptide well accorded with the corresponding SI peptide. The amount of each peptide was calculated on the basis of the peak area of each SI peptide. As a result, 15 phosphopeptides were successfully quantified (Figure 2, Table 4). Among them, a significant difference in the phosphopeptide level between high- and low-risk groups was observed in sister chromatid cohesion protein PDS5 homologue A T1208, C–C chemokine receptor type 1 S352, LIM domain-only protein 7 S417 and dolichyl-P-Man:Man(5)GlcNAc(2)-PP-dolichyl mannosyltransferase S13 ($p < 0.05$) (Figure 2A). Eight phosphopeptides showed a difference between the two groups, although not significantly ($p < 0.2$). This included shroom family member 3 protein S439, cell division protein kinase 1/2/3 Y15, cell division protein kinase 1/2/3 T14, interferon-induced GTP-binding protein Mx1 S4, 60S ribosomal protein L23a S43, DNA replication licensing factor MCM2 S139, mucin-1 S1227 and myelin protein zero-like protein 1 Y263 (Figure 2B). Three phosphopeptides, plakophilin-2 S151, keratin, type II cytoskeletal 8 S291 and InaD-like protein S645, showed no significant difference between the two groups (Figure 2C).

To examine the correlation of the quantitation data between SRM and iTRAQ analyses, we compared the expression level of phosphopeptides obtained by SRM with that of iTRAQ. Figure 3 shows examples of the correlation. Cell division protein kinase 1/2/3 T14, LIM domain-only protein 7 S417, sister chromatid cohesion protein PDS5 homologue A T1208, C–C chemokine receptor type 1 S352, DNA replication licensing factor MCM2 S139, cell division protein kinase 1/2/3 Y15, myelin protein zero-like protein 1 Y263, keratin type II cytoskeletal 8 S291, plakophilin-2 S151 and shroom family member 3 protein S439

were highly correlated between iTRAQ and SRM ($r^2 > 0.6$), whereas 60S ribosomal protein L23a S43, interferon-induced GTP-binding protein Mx1 S4 and dolichyl-P-Man:Man(5)-GlcNAc(2)-PP-dolichyl mannosyltransferase S13 were less well correlated ($r^2 > 0.4$ to < 0.6), and InaD-like protein S645 and mucin-1 S1227 showed no correlation. The reason for this discrepancy might be due to the low abundance of phosphopeptides, small sample size, heterogeneity of tissue samples, and complicated procedure of phosphoproteomic analysis without suitable internal standards (also see the Discussion section).

Since the Mucin-1 expression level has been reported to inversely correlate with recurrence and distal metastasis, we examined Mucin-1 protein expression in breast cancer tissues in high- and low-risk recurrence groups because the difference in the Mucin-1 phosphoprotein level might be due to its protein level. Mucin-1 is expressed as a stable heterodimer after translation and is cleaved into two subunits, N-terminal and C-terminal subunits.⁴⁵ Since the Mucin-1 phosphopeptide identified in our analysis is located in the C-terminal subunit, we used a monoclonal antibody against the C-terminus that has previously been reported (Ab-5).⁴⁵ Increased expression of Mucin-1 protein was observed in some breast cancer tissues, although the protein expression did not correlate with the phosphopeptide levels observed (Supporting Information Figure S3). Thus, the difference in Mucin-1 phosphopeptide levels was not due to Mucin-1 protein expression, and further evaluation of the phosphorylated Mucin-1 level is needed.

DISCUSSION

In this paper, we established a discovery-through-verification strategy for large-scale phosphoproteomic analysis using breast cancer tissues. By comprehensive quantitative analysis using iTRAQ, we identified 8309 phosphorylation sites on 3401 proteins, of which 3766 phosphopeptides (1927 phosphoproteins) were quantified and 133 phosphopeptides (131 phosphoproteins) were differentially expressed between high- and low-risk recurrence groups predicted by MammaPrint. Nineteen phosphopeptides were verified by SRM using stable isotope peptides, and 15 underwent successful SRM-based quantitation. These results suggest that large-scale phosphoproteome quantification coupled with SRM-based validation is a powerful tool for biomarker discovery using clinical samples.

The number of phosphorylation site identifications has exponentially increased since the mid-2000s,⁵¹ probably due to the improvement of phosphopeptide enrichment methods such as IMAC¹⁴ or TiO₂⁵² and antiphospho specific antibody.⁵³ A phosphoproteomic study of HeLa cells arrested in the G and mitotic phases of the cell cycle identified more than 65 000 phosphopeptides with a combination of phosphopeptide enrichment and strong cation exchange (SCX) chromatography.⁵⁴ Several phosphoproteomic studies using tissue samples have been reported and identified: 5195 phosphopeptides from the human dorsolateral prefrontal cortex³⁵ and 5698 phosphorylation sites from tumor tissues of melanoma model mice.²³ In the study, we were able to identify 8309 phosphorylation sites, far beyond the number of previous phosphoproteomic reports using tissue samples.

iTRAQ quantitative analysis is very useful for comprehensive analysis of the phosphoproteome in tissue samples. In our analysis, the ratios (the ratio of high-risk to low-risk group's average) of completely digested peptides were mostly similar to those of incompletely digested peptides with the same

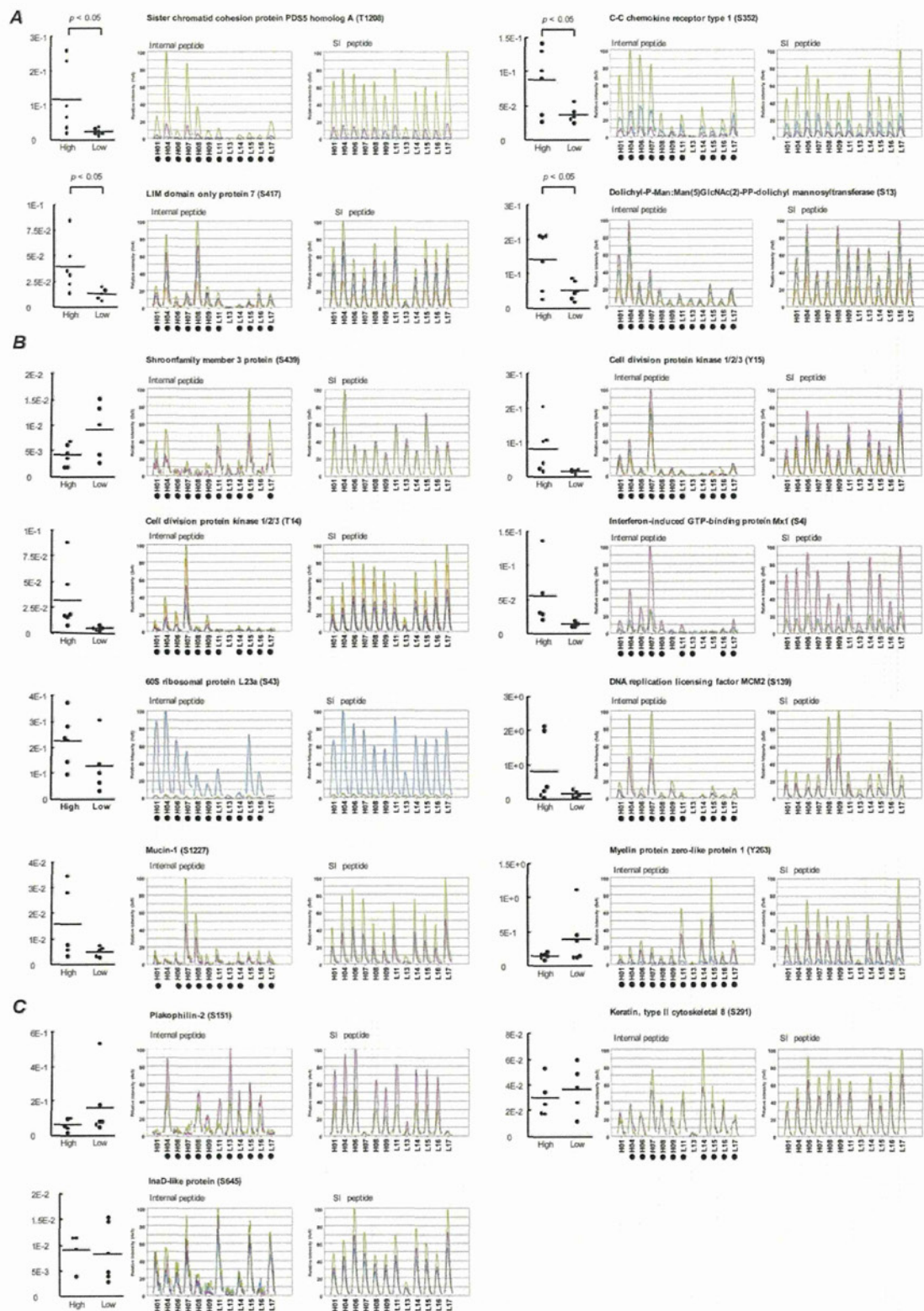


Figure 2. Relative quantitation of phosphopeptides between two groups from breast tissues by SRM. The scatter plots indicate the peak area ratio of the internal peptide to SI peptide and each horizontal bar indicates the mean value. Y-axis shows the normalized peak area. The “internal peptide” and “SI peptide” are based on the transition from internal peptides and SI peptides, respectively. (A) indicates significant difference groups ($p < 0.05$), (B) different propensity ($p > 0.05$, < 0.2), and (C) no significant difference between two groups ($p > 0.2$). Closed circle indicates samples that were satisfactorily quantified.

Table 4. SRM-Based Quantification of Phosphopeptides^a

gene symbol	Uniprot accession	protein name	targeted phosphopeptide	phosphorylated site	high/low ratio	T. TEST	area ratio (unlabeled/stable-isotope labeled peptide)												
							H01	H04	H06	H07	H08	H09	L11	L13	L14	L15	L16	L17	
RPL23A	P62750	60S ribosomal protein L23a	IRTPSPPTFR	S43	0.20	0.149	3.8×10^{-1}	2.8×10^{-1}	2.4×10^{-1}	2.3×10^{-1}	1.4×10^{-1}	9.5×10^{-2}	1.0×10^{-1}	6.5×10^{-2}	3.2×10^{-2}	3.1×10^{-1}	1.4×10^{-1}	ND	
MX1	P20591	Interferon-induced GTP-binding protein Mx1	WpSEVDIAK	S4	3.94	0.123	2.1×10^{-2}	6.0×10^{-2}	2.9×10^{-2}	1.4×10^{-1}	3.2×10^{-2}	ND	1.1×10^{-2}	1.5×10^{-2}	ND	ND	2.0×10^{-2}	1.0×10^{-2}	
CDK1 CDK2 CDK3	P06493 P24941 Q00526	Cell division protein kinase 1/2/3	IGEGpTYGWYK	T14	6.99	0.077	1.9×10^{-2}	4.8×10^{-2}	1.7×10^{-2}	8.9×10^{-2}	7.2×10^{-3}	1.6×10^{-2}	5.1×10^{-3}	ND	5.4×10^{-3}	7.5×10^{-3}	2.8×10^{-3}	2.4×10^{-3}	
LMO7	Q8WW11	LIM domain only protein 7	pSYTSDLOK	S417	3.07	0.048	2.2×10^{-2}	5.0×10^{-2}	1.4×10^{-1}	3.5×10^{-2}	8.5×10^{-2}	3.2×10^{-2}	1.3×10^{-2}	ND	6.4×10^{-3}	9.0×10^{-3}	2.0×10^{-2}	1.7×10^{-2}	
ALGS	Q92685	Dolichyl-P-Man ₅ Man(5)GlcNAc(2)-PP-dolichyl mannosyltransferase	SGpSAAQAEGLCCK	S13	2.74	0.049	2.1×10^{-1}	2.1×10^{-1}	1.4×10^{-1}	2.1×10^{-1}	5.1×10^{-2}	2.6×10^{-2}	4.5×10^{-2}	2.8×10^{-2}	5.1×10^{-2}	6.0×10^{-2}	1.7×10^{-2}	8.7×10^{-2}	
PDSSA	Q29RF7-1	Sister chromatid cohesion protein PDSS homologue A	IISVpTPVK	T1208	5.14	0.044	6.7×10^{-2}	2.3×10^{-1}	2.1×10^{-2}	2.6×10^{-1}	1.0×10^{-1}	3.6×10^{-2}	2.4×10^{-2}	1.1×10^{-1}	1.7×10^{-2}	3.1×10^{-2}	1.9×10^{-2}	3.7×10^{-2}	
CCR1	P32246	C-C chemokine receptor type 1	VSSTSPSTGEHELpSAGF	S352	2.34	0.046	1.3×10^{-1}	1.4×10^{-1}	9.0×10^{-2}	1.0×10^{-1}	3.8×10^{-2}	2.7×10^{-2}	3.4×10^{-2}	ND	3.1×10^{-2}	2.5×10^{-2}	4.2×10^{-2}	5.7×10^{-2}	
MCM2	O95297-1	DNA replication licensing factor MCM2	GLLYDpSDEEDEERPAR	S139	5.30	0.156	3.6×10^{-1}	2.0	2.5×10^{-1}	2.1	3.9×10^{-2}	1.3×10^{-1}	1.3×10^{-1}	ND	9.4×10^{-2}	2.8×10^{-1}	3.3×10^{-2}	2.3×10^{-1}	
CDK1 CDK2 CDK3	P60493 P24941 Q00526	Cell division protein kinase 1/2/3	IGEGTpyGWYK	Y15	5.09	0.074	1.0×10^{-1}	1.1×10^{-1}	1.5×10^{-2}	2.1×10^{-1}	2.5×10^{-2}	4.0×10^{-2}	1.5×10^{-2}	ND	6.3×10^{-3}	1.8×10^{-2}	2.1×10^{-2}	2.0×10^{-2}	
MPZL1	O95297-1	Myelin protein zero-like protein 1	SESVVpYADIR	Y263	0.39	0.183	1.2×10^{-1}	2.1×10^{-1}	1.7×10^{-1}	1.5×10^{-1}	9.7×10^{-2}	1.7×10^{-1}	4.6×10^{-1}	1.5×10^{-1}	3.8×10^{-1}	1.1	1.3×10^{-1}	1.3×10^{-1}	
KRT8	P05787	Keratin, type II cytoskeletal 8	YEELQpSLAGK	S291	0.81	0.533	ND	3.5×10^{-2}	1.8×10^{-2}	5.4×10^{-2}	2.6×10^{-2}	1.9×10^{-2}	3.9×10^{-2}	ND	6.6×10^{-3}	4.9×10^{-2}	2.7×10^{-2}	1.2×10^{-2}	
MUC1	P15941-1	Mucin-1	YVPPSSTDRpSPYEK	S1227	3.10	0.170	0.63	0.46	0.72			0.64	1.02	1.1	2.03	1.84	1.28		
PKP2	Q99959-1	Plakophilin-2	LELpSPDSSPER	S151	0.37	0.243	0.07	0.27	0.16	0.48	0.34	0.3	1.11	0.32	0.22	5.96	0.84	0.78	
INADL	Q8NI35-1	InaD like protein	LFDDApSVDEPR	S645	1.08	0.834	1.1×10^{-2}	9.3×10^{-3}	4.0×10^{-3}	1.1×10^{-2}	ND	ND	1.5×10^{-2}	4.8×10^{-3}	3.9×10^{-3}	1.5×10^{-2}	2.9×10^{-3}	8.5×10^{-3}	
SHROOM3	Q8TF72-1	shroom family member 3 protein	pSPLNSPPVKPK	S439	0.46	0.071	6.9×10^{-3}	4.7×10^{-3}	1.9×10^{-3}	3.7×10^{-3}	1.9×10^{-3}	6.3×10^{-3}	1.0×10^{-3}	2.8×10^{-3}	4.3×10^{-3}	1.3×10^{-3}	ND	1.5×10^{-3}	

^aND: not detected.

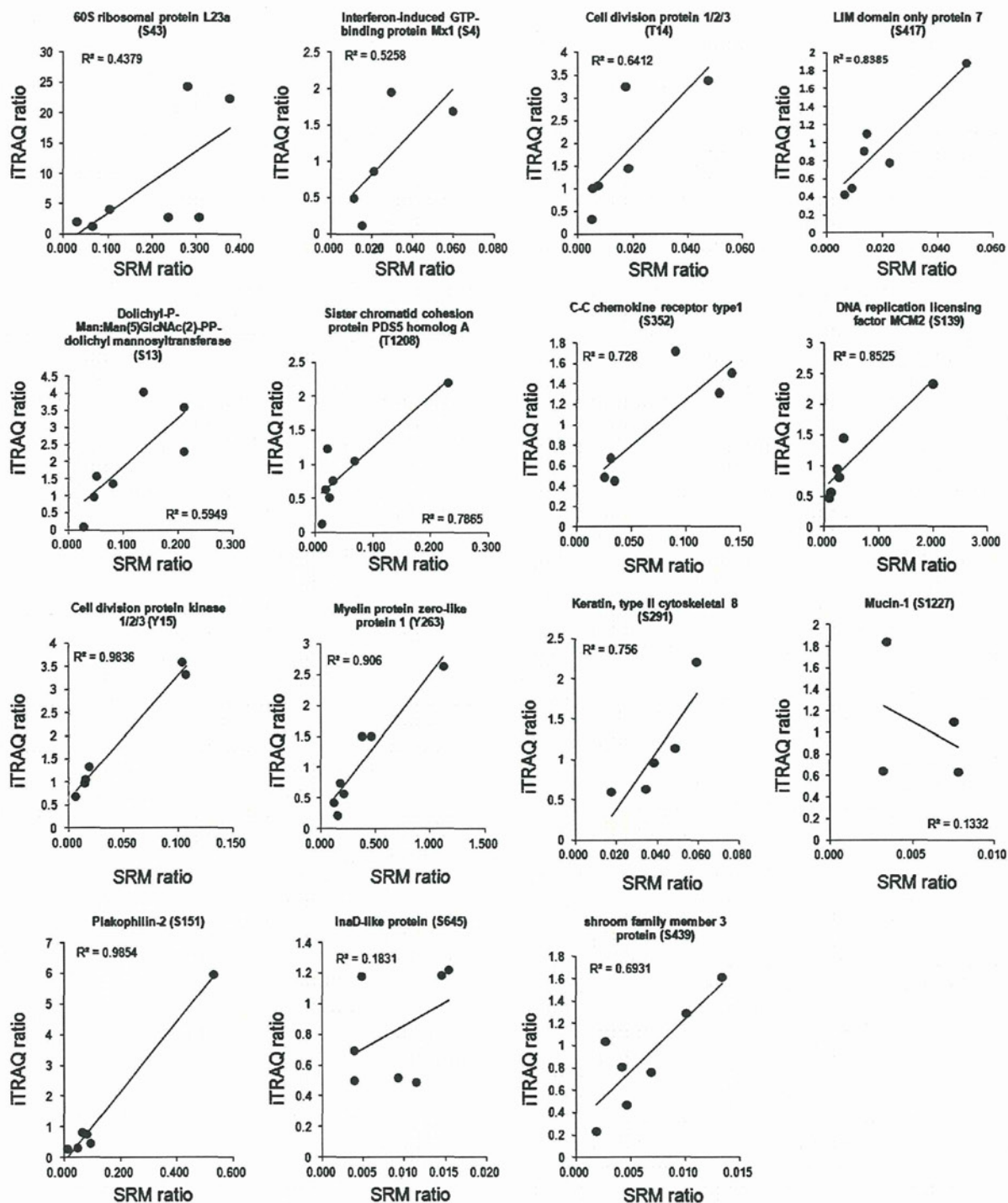


Figure 3. Linear regression comparing peptide ratio results obtained by iTRAQ and SRM assay. The iTRAQ and SRM ratios were plotted on each graph. Each data point represents a given peptide ratio in the same samples, which were quantified by either iTRAQ or SRM assay. Correlation coefficients are shown in plots.

phosphorylation site. For example, FVpSEGDGGR (fold change: 0.26) and RFVpSEGDGGR (0.48) peptides with pS457 of programmed cell death protein 4 and AGGSAALpSPSK (2.49) and AGGSAAALpSPSK (2.08) peptides with pS31 of Histone H1x both showed significant

differences between high- and low-risk groups (Supporting Information Table S4), which would indicate that our large-scale phosphoproteomic analysis had sufficient quantitative reproducibility to search for putative phosphoprotein biomarkers.

Verification of the phosphorylation state is essential in the search for phospho-biomarkers. If specific and well-characterized antibodies for these candidates are available, the validation step could be performed easily using Western blotting and ELISA. However, highly specific antibodies for most phosphoproteins are not available, and the development of good antibodies that recognize a specific phosphorylation frame is a cumbersome, expensive and time-consuming process that requires a priori knowledge of the protein and its phosphorylation sites. On the other hand, SRM does not require antibodies and is able to validate multiple phosphorylation sites within a single run. Recently, SRM analysis was used to validate the evidence for a large-scale proteome;^{55–57} however, phosphopeptide SRM has only been performed for specific protein phosphorylation such as Akt,⁵⁸ Lyn,⁵⁹ EGFR⁶⁰ or tyrosine phosphorylated peptides after EGF treatment.⁶¹ In this study, we selected and validated 19 phosphopeptides from 133 biomarker candidate phosphopeptides of breast cancer tissue discovered by iTRAQ-based phosphoproteomics. To our knowledge, this study is the first to validate phosphopeptides discovered by large-scale phosphoproteomic analysis using SRM.

Recently, several reports identified biomarker candidates by quantitative shotgun proteomics and subsequent validation by SRM,^{57,62} but these studies carried out the SRM assay without SI peptides. Although this method has the advantage of reducing the cost and time for SI peptide synthesis, difficulties occur in SRM analysis without internal standards, which provide the correct retention time for target peptides and verify the specificity of the analyte.⁵⁶ Also, the use of SI peptide provides the most favorable SRM information, such as the highest intensity fragment ions for each peptide. Thus, inclusion of SI peptides as an internal control is indispensable, especially for quantitation of low-abundance proteins such as phosphopeptide. Whiteaker et al. pointed out that the choice of candidates for quantitative SRM assay development was limited to the most abundant proteins or peptides without internal standards.⁵⁶ Our successful quantitation of low abundant phosphopeptides was largely a result of the inclusion of SI peptides.

In this study, only four of 15 potential biomarker candidate phosphopeptides quantified by iTRAQ showed a significant difference between high- and low-risk groups of breast cancer (Figure 2) and quantification of the amount of phosphopeptides by iTRAQ and SRM was not always correlated (Figure 3). Several reasons could be considered for the discrepancy. First, the sample size used for both discovery and verification was very small. In addition to the four phosphopeptides with a significant difference obtained by our SRM analysis, eight candidate phosphopeptides showed quite different expressions, although not significantly, between high- and low-risk groups. If we could increase the number of samples, more biomarker candidate phosphopeptides identified by the discovery approach could be verified. Second, quantitative variation might be generated in the discovery phase of phosphoproteomics. This includes one additional step of phosphopeptide enrichment by IMAC as compared with the usual iTRAQ method, which might create such variation. Moreover, the heterogeneity of cancer tissue samples could further highlight quantitative variation in a step of phosphopeptide enrichment. This is evidenced by the fact that good reproducibility and correlation were obtained between the quantitation of phosphopeptides by iTRAQ and SRM when their analysis was performed using samples prepared from cell lysate (data not shown). Phosphopeptide enrichment might be more sensitive to the composition of the

sample and the solution used for lysis or digestion of protein extracts; therefore, validation by SRM analysis is very important for the biomarker candidate phosphopeptides discovered by iTRAQ analysis combined with IMAC. Third, the endogenous phosphopeptide level is near the limit of quantitation so that the number of phosphopeptides quantified even with highly sensitive SRM was not accurate enough. We have observed that iTRAQ-based discovery and SRM-based validation of biomarker candidates of membrane proteins obtained from breast cancer tissues were well correlated.⁶³ This was probably due to the abundance of membrane proteins as compared with phosphoprotein. Thus, further improvement of the sensitivity of SRM is needed for accurate quantitation of low-abundance protein such as phosphoprotein.

In conclusion, we performed a large-scale phosphoproteome quantification and subsequent SRM-based validation using breast cancer tissue samples. The significance of this study is to provide a strategy for the quantitation and validation of low-abundance phosphopeptides using the most recent proteomic technologies, which might lead to a fundamental shift from traditional validation using antibodies. Quantitation of phosphopeptides by SRM will be applied to examine various kinase activities and signaling pathways in cells in the near future.

■ ASSOCIATED CONTENT

📄 Supporting Information

Figure S1. Schematic workflow of iTRAQ analysis combined with IMAC for identification of potential biomarkers and SRM analysis combined with IMAC for validation. Figure S2. Venn diagram of the phosphopeptides identified in the four experiments of iTRAQ-based proteomic analysis. Figure S3. Expression of Mucin-1 protein in breast cancer tissues. Table S1. Patient information in experiment. Table S2. Identified phosphopeptides. Table S3. Quantified phosphopeptides. Table S4. Phosphopeptides with significant difference between two groups by iTRAQ analysis. Table S5. Transition list of target phosphopeptides. This material is available free of charge via the Internet at <http://pubs.acs.org>.

■ AUTHOR INFORMATION

Corresponding Author

*Tel: +81-72-641-9862. Fax: +81-72-641-9861. E-mail: tomonaga@nibio.go.jp.

Author Contributions

#Ryohei Narumi and Tatsuo Murakami contributed equally to this paper.

Notes

The authors declare no competing financial interest.

■ ACKNOWLEDGMENTS

This work was supported by a Grant-in-Aid for Research on Biological Markers for New Drug Development H20-0005 to T.T. from the Ministry of Health, Labour and Welfare of Japan and by Grant-in-Aid 21390354 to T.T. from the Ministry of Education, Science, Sports and Culture of Japan.

■ ABBREVIATIONS

iTRAQ, isobaric peptide tags for relative and absolute quantification; SRM, selected reaction monitoring; IMAC, immobilized metal affinity chromatography; SI peptide, stable isotope-labeled peptide; SCX, strong cation exchange; CID,

collision-induced dissociation; HCD, higher energy collision-induced dissociation; LC-MS/MS, liquid chromatography-tandem mass spectrometry; CE, collision energy; LTQ, linear ion trap; fwhm, full width at half-maximum; FDR, false discovery rate

REFERENCES

- (1) Hanahan, D.; Weinberg, R. A. The hallmarks of cancer. *Cell* **2000**, *100* (1), 57–70.
- (2) Kaminska, B. MAPK signalling pathways as molecular targets for anti-inflammatory therapy—from molecular mechanisms to therapeutic benefits. *Biochim. Biophys. Acta* **2005**, *1754* (1–2), 253–62.
- (3) Peifer, C.; Wagner, G.; Laufer, S. New approaches to the treatment of inflammatory disorders small molecule inhibitors of p38 MAP kinase. *Curr. Top. Med. Chem.* **2006**, *6* (2), 113–49.
- (4) White, M. F. Regulating insulin signaling and beta-cell function through IRS proteins. *Can. J. Physiol. Pharmacol.* **2006**, *84* (7), 725–37.
- (5) Neville, D. C.; Rozanas, C. R.; Price, E. M.; Gruis, D. B.; Verkman, A. S.; Townsend, R. R. Evidence for phosphorylation of serine 753 in CFTR using a novel metal-ion affinity resin and matrix-assisted laser desorption mass spectrometry. *Protein Sci.* **1997**, *6* (11), 2436–45.
- (6) Ong, S. E.; Blagoev, B.; Kratchmarova, I.; Kristensen, D. B.; Steen, H.; Pandey, A.; Mann, M. Stable isotope labeling by amino acids in cell culture, SILAC, as a simple and accurate approach to expression proteomics. *Mol. Cell. Proteomics* **2002**, *1* (5), 376–86.
- (7) Ross, P. L.; Huang, Y. N.; Marchese, J. N.; Williamson, B.; Parker, K.; Hattan, S.; Khainovski, N.; Pillai, S.; Dey, S.; Daniels, S.; Purkayastha, S.; Juhasz, P.; Martin, S.; Bartlet-Jones, M.; He, F.; Jacobson, A.; Pappin, D. J. Multiplexed protein quantitation in *Saccharomyces cerevisiae* using amine-reactive isobaric tagging reagents. *Mol. Cell. Proteomics* **2004**, *3* (12), 1154–69.
- (8) Collins, M. O.; Yu, L.; Coba, M. P.; Husi, H.; Campuzano, I.; Blackstock, W. P.; Choudhary, J. S.; Grant, S. G. Proteomic analysis of in vivo phosphorylated synaptic proteins. *J. Biol. Chem.* **2005**, *280* (7), 5972–82.
- (9) Molina, H.; Horn, D. M.; Tang, N.; Mathivanan, S.; Pandey, A. Global proteomic profiling of phosphopeptides using electron transfer dissociation tandem mass spectrometry. *Proc. Natl. Acad. Sci. U. S. A.* **2007**, *104* (7), 2199–204.
- (10) Wissing, J.; Jansch, L.; Nimtz, M.; Dieterich, G.; Hornberger, R.; Keri, G.; Wehland, J.; Daub, H. Proteomics analysis of protein kinases by target class-selective prefractionation and tandem mass spectrometry. *Mol. Cell. Proteomics* **2007**, *6* (3), 537–47.
- (11) Villen, J.; Beausoleil, S. A.; Gerber, S. A.; Gygi, S. P. Large-scale phosphorylation analysis of mouse liver. *Proc. Natl. Acad. Sci. U. S. A.* **2007**, *104* (5), 1488–93.
- (12) Ballif, B. A.; Villen, J.; Beausoleil, S. A.; Schwartz, D.; Gygi, S. P. Phosphoproteomic analysis of the developing mouse brain. *Mol. Cell. Proteomics* **2004**, *3* (11), 1093–101.
- (13) Beausoleil, S. A.; Jedrychowski, M.; Schwartz, D.; Elias, J. E.; Villen, J.; Li, J.; Cohn, M. A.; Cantley, L. C.; Gygi, S. P. Large-scale characterization of HeLa cell nuclear phosphoproteins. *Proc. Natl. Acad. Sci. U. S. A.* **2004**, *101* (33), 12130–5.
- (14) Ficarro, S. B.; McClelland, M. L.; Stukenberg, P. T.; Burke, D. J.; Ross, M. M.; Shabanowitz, J.; Hunt, D. F.; White, F. M. Phosphoproteome analysis by mass spectrometry and its application to *Saccharomyces cerevisiae*. *Nat. Biotechnol.* **2002**, *20* (3), 301–5.
- (15) Lee, J.; Xu, Y.; Chen, Y.; Sprung, R.; Kim, S. C.; Xie, S.; Zhao, Y. Mitochondrial phosphoproteome revealed by an improved IMAC method and MS/MS/MS. *Mol. Cell. Proteomics* **2007**, *6* (4), 669–76.
- (16) Moser, K.; White, F. M. Phosphoproteomic analysis of rat liver by high capacity IMAC and LC-MS/MS. *J. Proteome Res.* **2006**, *5* (1), 98–104.
- (17) Trinidad, J. C.; Specht, C. G.; Thalhammer, A.; Schoepfer, R.; Burlingame, A. L. Comprehensive identification of phosphorylation sites in postsynaptic density preparations. *Mol. Cell. Proteomics* **2006**, *5* (5), 914–22.
- (18) Li, X.; Gerber, S. A.; Rudner, A. D.; Beausoleil, S. A.; Haas, W.; Villen, J.; Elias, J. E.; Gygi, S. P. Large-scale phosphorylation analysis of alpha-factor-arrested *Saccharomyces cerevisiae*. *J. Proteome Res.* **2007**, *6* (3), 1190–7.
- (19) Matsuoka, S.; Ballif, B. A.; Smogorzewska, A.; McDonald, E. R., 3rd; Hurov, K. E.; Luo, J.; Bakalarski, C. E.; Zhao, Z.; Solimini, N.; Lerenthal, Y.; Shiloh, Y.; Gygi, S. P.; Elledge, S. J. ATM and ATR substrate analysis reveals extensive protein networks responsive to DNA damage. *Science* **2007**, *316* (5828), 1160–6.
- (20) Olsen, J. V.; Blagoev, B.; Gnäd, F.; Macek, B.; Kumar, C.; Mortensen, P.; Mann, M. Global, in vivo, and site-specific phosphorylation dynamics in signaling networks. *Cell* **2006**, *127* (3), 635–48.
- (21) Trinidad, J. C.; Thalhammer, A.; Specht, C. G.; Lynn, A. J.; Baker, P. R.; Schoepfer, R.; Burlingame, A. L. Quantitative analysis of synaptic phosphorylation and protein expression. *Mol. Cell. Proteomics* **2008**, *7* (4), 684–96.
- (22) Nguyen, V.; Cao, L.; Lin, J. T.; Hung, N.; Ritz, A.; Yu, K.; Jianu, R.; Ulin, S. P.; Raphael, B. J.; Laidlaw, D. H.; Brossay, L.; Salomon, A. R. A new approach for quantitative phosphoproteomic dissection of signaling pathways applied to T cell receptor activation. *Mol. Cell. Proteomics* **2009**, *8* (11), 2418–31.
- (23) Zanivan, S.; Gnäd, F.; Wickstrom, S. A.; Geiger, T.; Macek, B.; Cox, J.; Fassler, R.; Mann, M. Solid tumor proteome and phosphoproteome analysis by high resolution mass spectrometry. *J. Proteome Res.* **2008**, *7* (12), 5314–26.
- (24) Anderson, N. L. The roles of multiple proteomic platforms in a pipeline for new diagnostics. *Mol. Cell. Proteomics* **2005**, *4* (10), 1441–4.
- (25) Lange, V.; Malmstrom, J. A.; Didion, J.; King, N. L.; Johansson, B. P.; Schafer, J.; Rameseder, J.; Wong, C. H.; Deutsch, E. W.; Brusniak, M. Y.; Buhlmann, P.; Bjorck, L.; Domon, B.; Aebersold, R. Targeted quantitative analysis of *Streptococcus pyogenes* virulence factors by multiple reaction monitoring. *Mol. Cell. Proteomics* **2008**, *7* (8), 1489–500.
- (26) Kuhn, E.; Wu, J.; Karl, J.; Liao, H.; Zolg, W.; Guild, B. Quantification of C-reactive protein in the serum of patients with rheumatoid arthritis using multiple reaction monitoring mass spectrometry and ¹³C-labeled peptide standards. *Proteomics* **2004**, *4* (4), 1175–86.
- (27) Anderson, L.; Hunter, C. L. Quantitative mass spectrometric multiple reaction monitoring assays for major plasma proteins. *Mol. Cell. Proteomics* **2006**, *5* (4), 573–88.
- (28) Keshishian, H.; Addona, T.; Burgess, M.; Kuhn, E.; Carr, S. A. Quantitative, multiplexed assays for low abundance proteins in plasma by targeted mass spectrometry and stable isotope dilution. *Mol. Cell. Proteomics* **2007**, *6* (12), 2212–29.
- (29) Keshishian, H.; Addona, T.; Burgess, M.; Mani, D. R.; Shi, X.; Kuhn, E.; Sabatine, M. S.; Gerszten, R. E.; Carr, S. A. Quantification of cardiovascular biomarkers in patient plasma by targeted mass spectrometry and stable isotope dilution. *Mol. Cell. Proteomics* **2009**, *8* (10), 2339–49.
- (30) van 't Veer, L. J.; Dai, H.; van de Vijver, M. J.; He, Y. D.; Hart, A. A.; Mao, M.; Peterse, H. L.; van der Kooy, K.; Marton, M. J.; Witteveen, A. T.; Schreiber, G. J.; Kerkhoven, R. M.; Roberts, C.; Linsley, P. S.; Bernards, R.; Friend, S. H. Gene expression profiling predicts clinical outcome of breast cancer. *Nature* **2002**, *415* (6871), 530–6.
- (31) Masuda, T.; Tomita, M.; Ishihama, Y. Phase transfer surfactant-aided trypsin digestion for membrane proteome analysis. *J. Proteome Res.* **2008**, *7* (2), 731–40.
- (32) Matsumoto, M.; Oyamada, K.; Takahashi, H.; Sato, T.; Hatakeyama, S.; Nakayama, K. I. Large-scale proteomic analysis of tyrosine-phosphorylation induced by T-cell receptor or B-cell receptor activation reveals new signaling pathways. *Proteomics* **2009**, *9* (13), 3549–63.

- (33) Kokubu, M.; Ishihama, Y.; Sato, T.; Nagasu, T.; Oda, Y. Specificity of immobilized metal affinity-based IMAC/C18 tip enrichment of phosphopeptides for protein phosphorylation analysis. *Anal. Chem.* **2005**, *77* (16), 5144–54.
- (34) Taus, T.; Kocher, T.; Pichler, P.; Paschke, C.; Schmidt, A.; Henrich, C.; Mechtler, K. Universal and confident phosphorylation site localization using phosphoRS. *J. Proteome Res.* **2011**, *10* (12), 5354–62.
- (35) Martins-de-Souza, D.; Guest, P. C.; Vanattou-Saifouline, N.; Rahmoune, H.; Bahn, S. Phosphoproteomic differences in major depressive disorder postmortem brains indicate effects on synaptic function. *Eur. Arch. Psychiatry Clin. Neurosci.* **2012**.
- (36) Jarvinen, T. A.; Tanner, M.; Barlund, M.; Borg, A.; Isola, J. Characterization of topoisomerase II alpha gene amplification and deletion in breast cancer. *Genes, Chromosomes Cancer* **1999**, *26* (2), 142–50.
- (37) Nielsen, K. V.; Muller, S.; Moller, S.; Schonau, A.; Balslev, E.; Knoop, A. S.; Ejlersten, B. Aberrations of ERBB2 and TOP2A genes in breast cancer. *Mol. Oncol.* **2010**, *4* (2), 161–8.
- (38) Futreal, P. A.; Liu, Q.; Shattuck-Eidens, D.; Cochran, C.; Harshman, K.; Tavtigian, S.; Bennett, L. M.; Haugen-Strano, A.; Swensen, J.; Miki, Y.; et al. BRCA1 mutations in primary breast and ovarian carcinomas. *Science* **1994**, *266* (5182), 120–2.
- (39) O'Donovan, P. J.; Livingston, D. M. BRCA1 and BRCA2: breast/ovarian cancer susceptibility gene products and participants in DNA double-strand break repair. *Carcinogenesis* **2010**, *31* (6), 961–7.
- (40) Castilla, L. H.; Couch, F. J.; Erdos, M. R.; Hoskins, K. F.; Calzone, K.; Garber, J. E.; Boyd, J.; Lubin, M. B.; Deshano, M. L.; Brody, L. C.; et al. Mutations in the BRCA1 gene in families with early-onset breast and ovarian cancer. *Nat. Genet.* **1994**, *8* (4), 387–91.
- (41) Kim, S. J.; Nakayama, S.; Miyoshi, Y.; Taguchi, T.; Tamaki, Y.; Matsushima, T.; Torikoshi, Y.; Tanaka, S.; Yoshida, T.; Ishihara, H.; Noguchi, S. Determination of the specific activity of CDK1 and CDK2 as a novel prognostic indicator for early breast cancer. *Ann. Oncol.* **2008**, *19* (1), 68–72.
- (42) Nasir, A.; Chen, D. T.; Gruidl, M.; Henderson-Jackson, E. B.; Venkataramu, C.; McCarthy, S. M.; McBride, H. L.; Harris, E.; Khakpour, N.; Yeatman, T. J. Novel molecular markers of malignancy in histologically normal and benign breast. *Pathol. Res. Int.* **2011**, *2011*, 489064.
- (43) Zheng, M. Z.; Zheng, L. M.; Zeng, Y. X. SCC-112 gene is involved in tumor progression and promotes the cell proliferation in G2/M phase. *J. Cancer Res. Clin. Oncol.* **2008**, *134* (4), 453–62.
- (44) Rakha, E. A.; Boyce, R. W.; Abd El-Rehim, D.; Kurien, T.; Green, A. R.; Paish, E. C.; Robertson, J. F.; Ellis, I. O. Expression of mucins (MUC1, MUC2, MUC3, MUC4, MUC5AC and MUC6) and their prognostic significance in human breast cancer. *Mod. Pathol.* **2005**, *18* (10), 1295–304.
- (45) Wei, X.; Xu, H.; Kufe, D. MUC1 oncoprotein stabilizes and activates estrogen receptor alpha. *Mol. Cell* **2006**, *21* (2), 295–305.
- (46) Mulligan, A. M.; Pinnaduwa, D.; Bane, A. L.; Bull, S. B.; O'Malley, F. P.; Andrulis, I. L. CK8/18 expression, the basal phenotype, and family history in identifying BRCA1-associated breast cancer in the Ontario site of the breast cancer family registry. *Cancer* **2011**, *117* (7), 1350–9.
- (47) Busch, T.; Milena, E.; Eiseler, T.; Joodi, G.; Temme, C.; Jansen, J.; Wichert, G. V.; Omary, M. B.; Spatz, J.; Seufferlein, T. Keratin 8 phosphorylation regulates keratin reorganization and migration of epithelial tumor cells. *J. Cell Sci.* **2012**, 2148–59.
- (48) Hu, Q.; Guo, C.; Li, Y.; Aronow, B. J.; Zhang, J. LMO7 mediates cell-specific activation of the Rho-myocardin-related transcription factor-serum response factor pathway and plays an important role in breast cancer cell migration. *Mol. Cell. Biol.* **2011**, *31* (16), 3223–40.
- (49) Merrell, K. W.; Crofts, J. D.; Smith, R. L.; Sin, J. H.; Kmetzsch, K. E.; Merrell, A.; Miguel, R. O.; Candelaria, N. R.; Lin, C. Y. Differential recruitment of nuclear receptor coregulators in ligand-dependent transcriptional repression by estrogen receptor-alpha. *Oncogene* **2011**, *30* (13), 1608–14.
- (50) Hartmaier, R. J.; Tchatchou, S.; Richter, A. S.; Wang, J.; McGuire, S. E.; Skaar, T. C.; Rae, J. M.; Hemminki, K.; Sutter, C.; Ditsch, N.; Bugert, P.; Weber, B. H.; Niederacher, D.; Arnold, N.; Varon-Mateeva, R.; Wappenschmidt, B.; Schmutzler, R. K.; Meindl, A.; Bartram, C. R.; Burwinkel, B.; Oesterreich, S. Nuclear receptor coregulator SNP discovery and impact on breast cancer risk. *BMC Cancer* **2009**, *9*, 438.
- (51) Lemeer, S.; Heck, A. J. The phosphoproteomics data explosion. *Curr. Opin. Chem. Biol.* **2009**, *13* (4), 414–20.
- (52) Larsen, M. R.; Thingholm, T. E.; Jensen, O. N.; Roepstorff, P.; Jorgensen, T. J. Highly selective enrichment of phosphorylated peptides from peptide mixtures using titanium dioxide microcolumns. *Mol. Cell. Proteomics* **2005**, *4* (7), 873–86.
- (53) Rush, J.; Moritz, A.; Lee, K. A.; Guo, A.; Goss, V. L.; Spek, E. J.; Zhang, H.; Zha, X. M.; Polakiewicz, R. D.; Comb, M. J. Immunoaffinity profiling of tyrosine phosphorylation in cancer cells. *Nat. Biotechnol.* **2005**, *23* (1), 94–101.
- (54) Dephoure, N.; Zhou, C.; Villen, J.; Beausoleil, S. A.; Bakalarski, C. E.; Elledge, S. J.; Gygi, S. P. A quantitative atlas of mitotic phosphorylation. *Proc. Natl. Acad. Sci. U. S. A.* **2008**, *105* (31), 10762–7.
- (55) Ostasiewicz, P.; Zielinska, D. F.; Mann, M.; Wisniewski, J. R. Proteome, phosphoproteome, and N-glycoproteome are quantitatively preserved in formalin-fixed paraffin-embedded tissue and analyzable by high-resolution mass spectrometry. *J. Proteome Res.* **2010**, *9* (7), 3688–700.
- (56) Whiteaker, J. R.; Lin, C.; Kennedy, J.; Hou, L.; Trute, M.; Sokal, I.; Yan, P.; Schoenherr, R. M.; Zhao, L.; Voytovich, U. J.; Kelly-Spratt, K. S.; Krasnoselsky, A.; Gafken, P. R.; Hogan, J. M.; Jones, L. A.; Wang, P.; Amon, L.; Chodosh, L. A.; Nelson, P. S.; McIntosh, M. W.; Kemp, C. J.; Paulovich, A. G. A targeted proteomics-based pipeline for verification of biomarkers in plasma. *Nat. Biotechnol.* **2011**, *29* (7), 625–34.
- (57) Addona, T. A.; Shi, X.; Keshishian, H.; Mani, D. R.; Burgess, M.; Gillette, M. A.; Clauser, K. R.; Shen, D.; Lewis, G. D.; Farrell, L. A.; Fifer, M. A.; Sabatine, M. S.; Gerszten, R. E.; Carr, S. A. A pipeline that integrates the discovery and verification of plasma protein biomarkers reveals candidate markers for cardiovascular disease. *Nat. Biotechnol.* **2011**, *29* (7), 635–43.
- (58) Atrih, A.; Turnock, D.; Sellar, G.; Thompson, A.; Feuerstein, G.; Ferguson, M. A.; Huang, J. T. Stoichiometric quantification of Akt phosphorylation using LC-MS/MS. *J. Proteome Res.* **2010**, *9* (2), 743–51.
- (59) Jin, L. L.; Tong, J.; Prakash, A.; Peterman, S. M.; St-Germain, J. R.; Taylor, P.; Trudel, S.; Moran, M. F. Measurement of protein phosphorylation stoichiometry by selected reaction monitoring mass spectrometry. *J. Proteome Res.* **2010**, *9* (5), 2752–61.
- (60) Tong, J.; Taylor, P.; Peterman, S. M.; Prakash, A.; Moran, M. F. Epidermal growth factor receptor phosphorylation sites Ser991 and Tyr998 are implicated in the regulation of receptor endocytosis and phosphorylations at Ser1039 and Thr1041. *Mol. Cell. Proteomics* **2009**, *8* (9), 2131–44.
- (61) Wolf-Yadlin, A.; Hautaniemi, S.; Lauffenburger, D. A.; White, F. M. Multiple reaction monitoring for robust quantitative proteomic analysis of cellular signaling networks. *Proc. Natl. Acad. Sci. U. S. A.* **2007**, *104* (14), S860–5.
- (62) Thingholm, T. E.; Bak, S.; Beck-Nielsen, H.; Jensen, O. N.; Gaster, M. Characterization of human myotubes from type 2 diabetic and nondiabetic subjects using complementary quantitative mass spectrometric methods. *Mol. Cell. Proteomics* **2011**, *10* (9), M110 006650.
- (63) Muraoka, S.; Kume, H.; Watanabe, S.; Adachi, J.; Kuwano, M.; Sato, M.; Kawasaki, N.; Kodera, Y.; Ishitobi, M.; Inaji, H.; Miyamoto, Y.; Kato, K.; Tomonaga, T. Strategy for SRM-based verification of biomarker candidates discovered by iTRAQ method in limited breast cancer tissue samples. *J. Proteome Res.* **2012**, *11* (8), 4201–10.

